Optik - International Journal for Light and Electron Optics 242 (2021) 167360

Contents lists available at ScienceDirect

Optik

journal homepage: www.elsevier.com/locate/ijleo

Original research article

In-situ measurement of aligning intensity and rotational temperature in field-free molecular alignment via white light generation

Necati Kaya [a,*], Gamze Kaya [b], Yakup Boran [c], Alexandre Kolomenski [d], Hans A. Schuessler [d]

[a] Department of Material Science and Engineering, Canakkale 18 Mart University, Terzioğlu Campus, Canakkale 17020, Turkey
[b] Department of Electric and Energy, Canakkale 18 Mart University, Terzioğlu Campus, Canakkale 17020, Turkey
[c] Department of Fundamental Sciences of Engineering, Sakarya University of Applied Sciences, Serdivan, Sakarya 54187, Turkey
[d] Department of Physics & Astronomy, Texas A&M University, College Station, TX 77843-4242, USA

ARTICLE INFO

Keywords:
Field-free molecular alignment
White-light generation
Pump-probe femtosecond pulses

ABSTRACT

We determine the aligning intensity and rotational temperature in field-free molecular alignment measured via white light signal. Relying on temporal dependencies of the time-resolved alignment signature obtained via white-light generation by femtosecond laser pulses in N_2 molecules, we derived the aligning pump intensity and rotational temperature using the occurrence times of the local alignment and anti-alignment around the half and full revivals. Results proved that the aligning intensity and rotational temperature can be obtained simultaneously by any two reverse local alignment extrema in the evolution of field-free molecular alignment.

1. Introduction

The alignment of molecules is critical for investigations of their structure and has been exploited in various experiments including x-ray [1] or electron diffraction in the gas phase [2], tomographic reconstruction of molecular orbitals [3], molecular fluorescence [4], spectral shift [5], and coherent emissions [6]. Field-free molecular alignment has also considerable interest owing to numerous applications [7,8]. These applications include imaging of molecular structures and molecular orbital reconstruction [3,9–12], measurements of vibrational and photoelectron dynamics in molecular frames [13–15], molecular scattering [16], chemical reaction control [17], selectively-controlled alignment of isotopes [18], nanolithography with molecular beams [19], ultrashort pulse compression [20,21], quantum information processing [22], charge migration [23], and high harmonic generation [24–28]. Molecular alignment plays a key role when controlling with laser fields optically induced dipole forces for molecules and their translational motions [29–31].

In addition, field-free molecular alignment can be used for better understanding of beam dynamics and filamentation control by optical refractive index modification during the beam propagation [21,32–37]. Studies of femtosecond laser filamentation resulting in white light generation at conditions of field-free alignment help to understand involved nonlinear optical processes, such as self-focusing, space-time wave packet evolution, self-phase modulation, intensity clamping and photoionization [38–41].

The field-free molecular alignment is highly sensitive to the aligning intensity and initial rotational temperature [42,43]. It was

* Corresponding author.
E-mail address: necatikaya@comu.edu.tr (N. Kaya).

https://doi.org/10.1016/j.ijleo.2021.167360
Received 21 March 2021; Received in revised form 1 June 2021; Accepted 1 June 2021
Available online 6 June 2021

shown that the aligning intensity and initial rotational temperature correlate with the width of the transients and the ratio between alignment (local maxima) and anti-alignment (local minima) peaks [44,45]. We note that unlike Ref. [45] our method relying on the measurements of the output of white light signal rather than on the yield of high harmonics works at lower intensities that are not supposed to produce ionization of the gas.

In this study, we aim to infer the aligning intensity and initial rotational temperature from the width of the transients and the signatures of the alignment and anti-alignment peaks in the evolution of field-free molecular alignment of femtosecond laser pulses via white light generation of the probing pulse. In our experiment, the pump pulse aligned molecules, and then a more intense probe pulse interacted with the aligned molecules to produce white-light generation [40]. The signal of the latter was measured for a varied delay between the aligning and probe pulses. With nitrogen molecules used in our proof-of-principle experiment, we show that the aligning intensity and initial rotational temperature is able to be obtained relying on local alignment and anti-alignment peaks in field-free molecular alignment measured via white-light generation signal. A similar measurement technique can be readily applied to other linear molecules.

2. Results and discussion

2.1. Experimental procedures

The experimental configuration is illustrated in Fig. 1, and is similar to the one in Ref [46], however here the polarizations of the pump and probe pulses are fixed to be parallel. We used a Ti:sapphire laser system with the central wavelength 800 nm, a pulse duration ~50 fs and 1 mJ per pulse energy at a 1 kHz repetition rate. The laser beam is split into two arms by a beam splitter to obtain the aligning and probe pulses. We used a translational stage (GTS150, ESP300, Newport) in one arm to adjust precisely the variable time delay between the pump and probe pulses. Minimum incremental motion of 100 nm allowed controlling the time delay with 0.67fs steps. A combination of a half-wave plate and a polarizer in the aligning pulse arm was used to adjust both polarization direction and the pump beam intensity. The two beams then were recombined and focused into a sealed gas cell. The gas cell was initially pumped down to 2×10^{-3} mbar, and then it was filled with pure nitrogen gas (99.9995%) to a pressure of 1 bar. We adjusted the peak pump pulse intensity to be just below the onset of the nonlinear spectral modification, which was still high enough for the molecular alignment. The intensity of the probe pulse in the focus was set to $\approx 10^{14}$ W/cm^2 to monitor the alignment using white light generation as an indicator. We note that for used laser parameters the ionization of N_2 gas by the probe pulse was negligibly small [47] for the considered here effects.

The white light was collected by a lens and directed onto a photodiode (PD300-UV). We used a shortpass filter to cut off the radiation around 800 nm from the incoming beams. The entire experiment was automated and controlled by a National Instruments DAQ card and a custom NI LabVIEW program.

2.2. Determining pump intensity and rotational temperature in field-free molecular alignment from time-dependent white-light signal

Here we show how the aligning pump intensity and initial rotational temperature of the gas molecular ensemble can be inferred from the occurrence times of the local alignment and anti-alignment peaks in the field-free molecular alignment. The expectation value of field-free molecular alignment is calculated by a double averaging procedure characterized by the quantity $<< \cos^2\theta >>$[48]. Firstly, for each initial molecular state $|\Phi(t=0)\rangle = |J_0 M_0\rangle$, the Schrödinger equation is solved and the expectation value of field-free molecular alignment for an initial state is calculated as

$$< \cos^2\theta >_{J_0 M_0}(t) = \left\langle \Phi_{J_0 M_0}(t) \middle| \cos^2\theta \middle| \Phi_{J_0 M_0}(t) \right\rangle \tag{1}$$

Secondly, since the gas is at thermal equilibrium before the interaction, averaging is performed taking into account Boltzmann

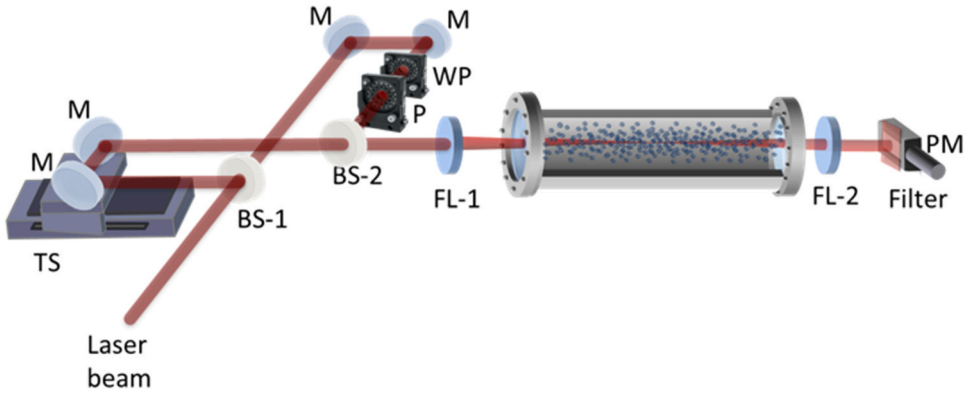

Fig. 1. The experimental layout. TS, translational stage; M, mirrors; BS-1,2, beam splitters; WP, half-wave plate; P, polarizer; FL-1,2, focusing lenses; PM, power meter.

distribution at the initial temperature T. Thus, the expectation value of molecular alignment of the ensemble at temperature T is calculated by averaging over the Boltzmann distribution of the rotational states including nuclear spin statistics of atoms constituting the molecule [48–50]:

$$\ll \cos^2\theta \gg (t) = \frac{\sum_{J_0} \sum_{M_0=-J_0}^{J_0} < \cos^2\theta >_{J_0 M_0}(t) g_{J_0} \exp(-BJ_0(J_0+1)/kT)}{\sum_{J_0} \sum_{M_0=-J_0}^{J_0} g_{J_0} \exp(-BJ_0(J_0+1)/kT)} \tag{2}$$

Here B is the rotational constant, g_{J_0} is statistical weight factor, k is the Boltzmann constant and J_0 is angular momentum quantum number.

For molecules with anisotropic polarizability, the aligning pump pulse induces a periodic change of the refractive index Δn for the probe pulse with polarization parallel to that of the aligning pulse [20].

$$\Delta n(t) = \frac{2\pi N}{n} \Delta\alpha \left(<< cos^2\theta >> (t) - 1/3 \right) \tag{3}$$

where $<< \cos^2\theta >> (t)$ is the time-dependent expectation value of field-free molecular alignment, N is the molecular number density, and n is the linear refractive index, $\Delta\alpha = \alpha_{\parallel} - \alpha_{\perp}$ ($\alpha_{\parallel}$, $\alpha_{\perp}$ are the components of the anisotropic polarizability for fields parallel and perpendicular to the molecular internuclear axis). Thus, the change of the refractive index is proportional to the alignment degree $< < \cos^2\theta >> (t)$ from the isotropic one (which is 1/3), so this difference in parentheses in Eq. (3) we call the alignment factor. Here we assume ionization to be negligible. Since $n - 1 = \alpha N/2$, where α is the average polarizability of the gas, the change of the refractive index is proportional to the alignment factor,

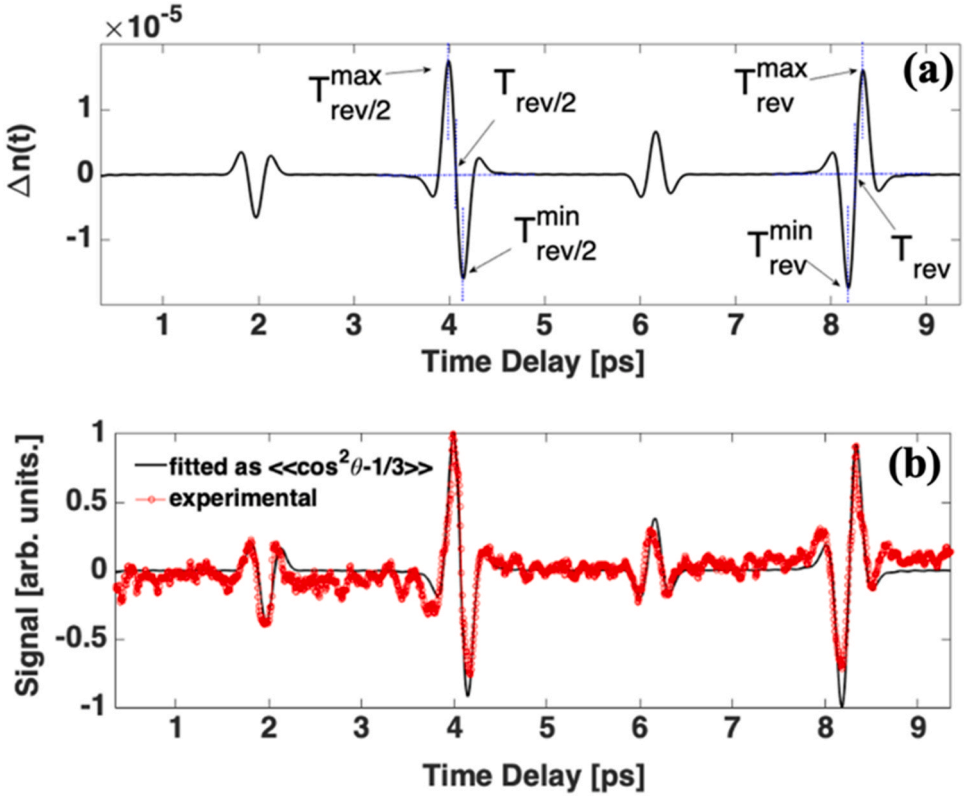

Fig. 2. (a) The calculated temporal evolution of the change of the refractive index at $I = 3 \times 10^{13}$ W/cm^2 and $T = 300$ K; this figure also shows the notations we are using for the temporal points of interest. (b) Measured white light signal (red circles) in N_2 from the molecular alignment process as a function of the time delay between the aligning pump and probe pulses with parallel polarizations. The black solid line is fitted as temporal evolution of the refractive index using Eqs. (2), (4). The occurrence times of the local extrema of white light signals around the half revival $\{T^{max}_{rev/2}, T^{\min}_{rev/2}\}$ and full revival $\{T^{max}_{rev}, T^{\min}_{rev}\}$ depend on the aligning pump intensity and the initial rotational temperature, while the middle points for revival signatures around $T_{rev}/2$ and T_{rev} are independent of these parameters. (For interpretation of the references to colour in this figure legend, the reader is referred to the web version of this article.)

$$\Delta n(t) = (4\pi)\frac{(n_0 - 1)}{n_0}\left(\frac{\Delta\alpha}{\alpha}\right)\left(<< cos^2\theta >> (t) - 1 \Big/ 3 \right) \quad (4)$$

and it can be used for the alignment monitoring [20,46].

For the experiment, we chose a linear symmetric top molecule, i.e N_2, having g_{J_0}=6 for even J's and g_{J_0}=3 for odd J's [51]. Fig. 2(a) presents the calculation of the temporal evolution of the refractive index change at I = 3 × 10^{13} W/cm^2 and T = 300 K, obtained with Eqs. (2), (4). The calculations show that the occurrence times of the local extrema of white light signals around the rotational revivals,

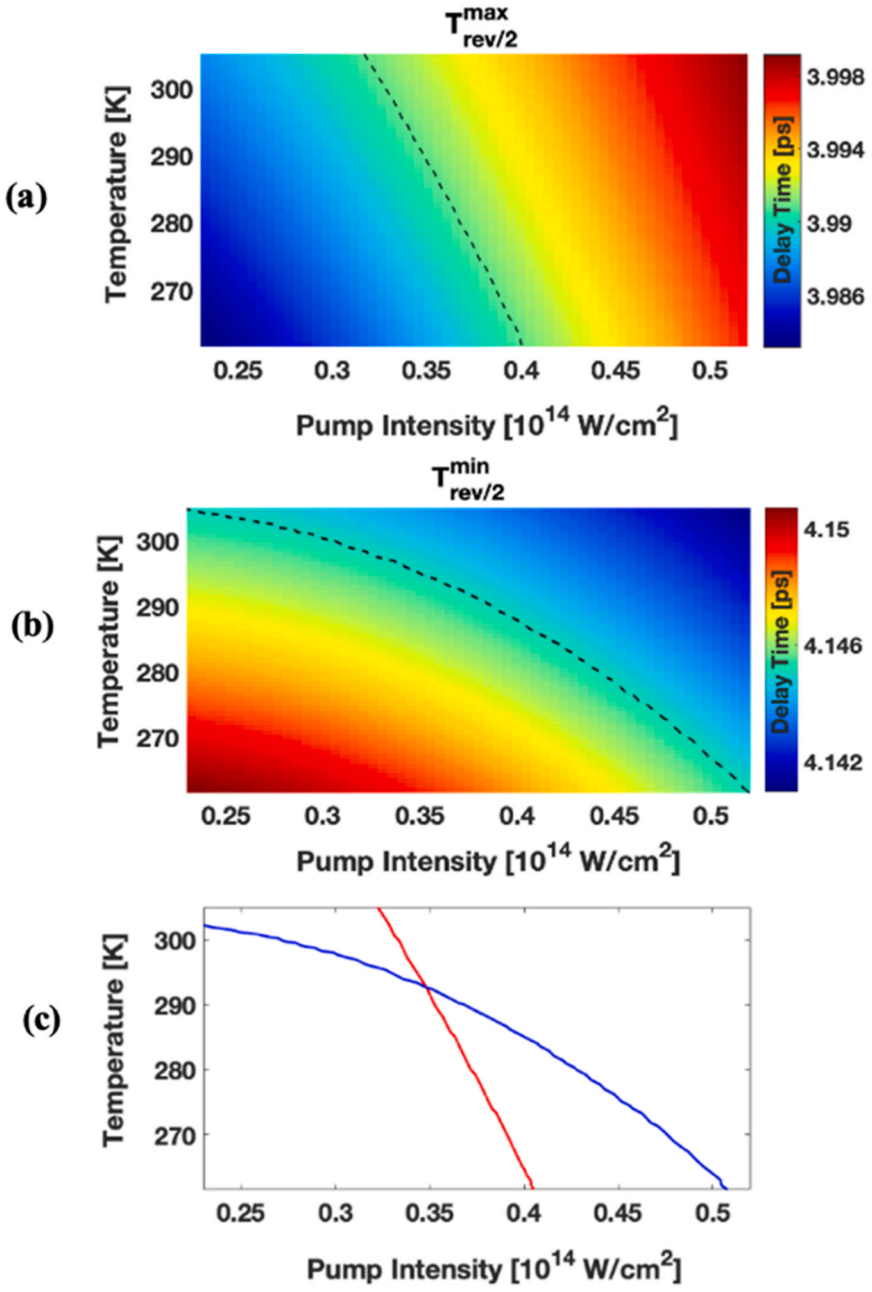

Fig. 3. (a) The occurrence time of the local maximum $T^{max}_{rev/2}$ around $T_{rev/2}$for N_2 as a function of the pump intensity and the rotational temperature. (b) Same as (a), but for the time of the local minimum $T^{min}_{rev/2}$. (c) Contour lines with $\{I, T\}$ pairs satisfying the experimentally determined value for $T^{max}_{rev/2}$ = 3.991 ps (red solid line) and $T^{min}_{rev/2}$ = 4.145 ps (blue solid line). These contour lines are also indicated in (a,b) as black dashed lines. The intersection of the contour lines determines the intensity and rotational temperature as $I = 3.48 \times 10^{13}$ W/cm^2 and $T = 292.5$ K. (For interpretation of the references to colour in this figure legend, the reader is referred to the web version of this article.)

$\{T^{max}_{rev/2}, T^{min}_{rev/2}\}$ and $\{T^{max}_{rev}, T^{min}_{rev}\}$ depend on the aligning intensity and the initial rotational temperature, which is important for further consideration. The middle points for revivals $T_{rev}/2$ and T_{rev} are determined by the rotational constant ($T_{rev} = 1/(2Bc)$, where c is the speed of light) and therefore are independent of I and T. The ratio of odd to even states for nitrogen gas of 1:2 leads to the appearance of somewhat reduced amplitudes of the alignment signatures at $T_{rev}/4$ and $3T_{rev}/4$, which however in view of their smaller amplitudes

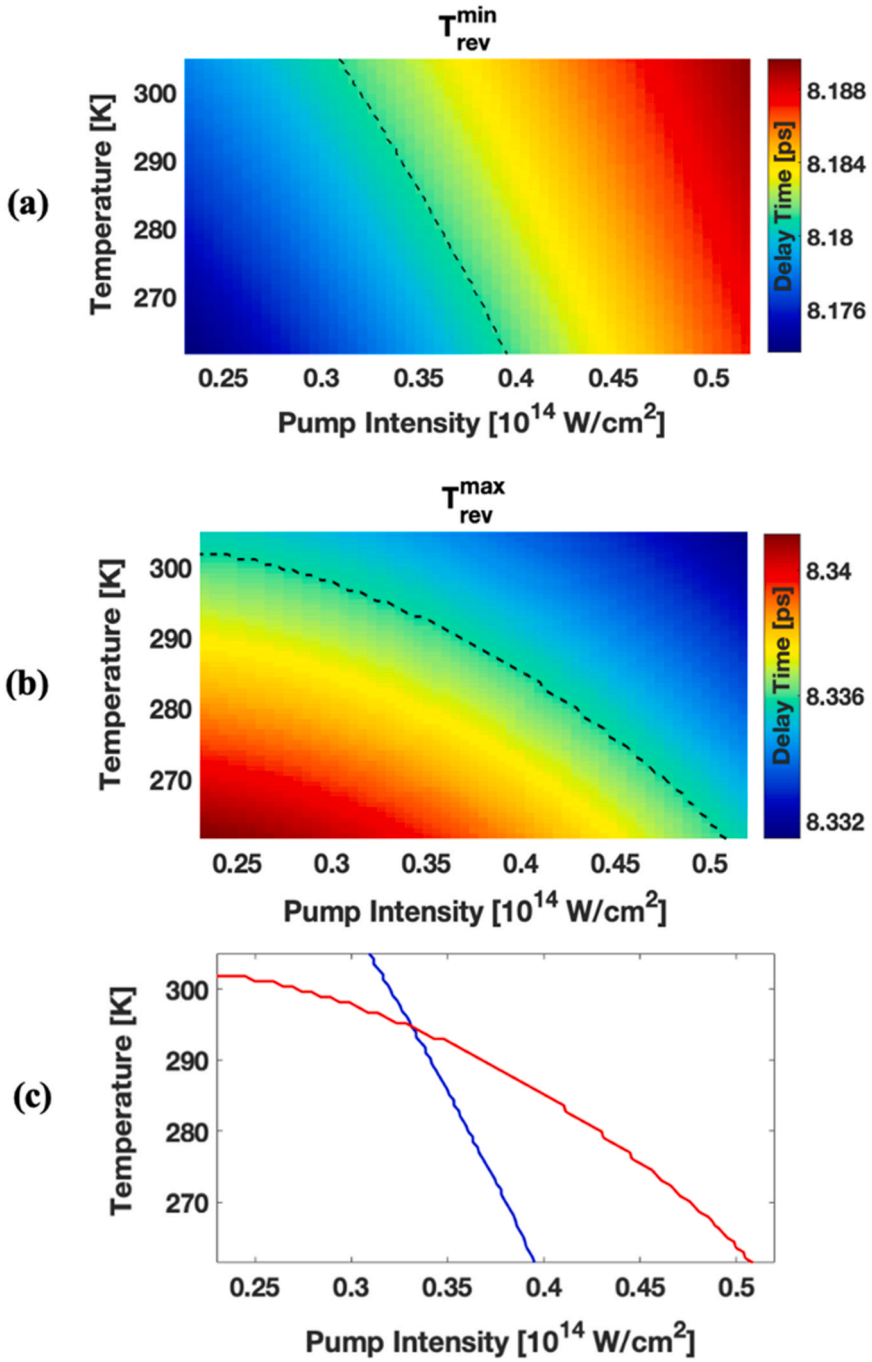

Fig. 4. (a) The occurrence time of the local minimum T^{min}_{rev} around T_{rev} for N_2 as a function of the aligning pump intensity and rotational temperature. (b) Same as (a), but for the occurrence time of the local maximum T^{max}_{rev} around T_{rev}. (c) Contour lines with $\{I, T\}$ pairs satisfying the experimentally determined value $T^{min}_{rev} = 8.181$ ps (blue solid line) and the same for $T^{max}_{rev} = 8.336$ ps (red solid line). These contour lines are also indicated in (a,b) as black dashed lines. The intersection of the contour lines gives the aligning intensity and initial rotational temperature as $I = 3.33 \times 10^{13}$ W/cm^2 and $T = 293.9$ K. (For interpretation of the references to colour in this figure legend, the reader is referred to the web version of this article.)

further will not be discussed.

The measured white-light signal (red circles) dependent on the pump-probe time-delay for N_2 molecules is shown in Fig. 2(b). The experimental data were fitted with the dependence calculated from Eqs. (2), (4), as shown by the black solid line in Fig. 2(b). The local alignment and anti-alignment peaks can be observed at the full and half revivals around 8.3 ps (T_{rev}) and 4.1 ps ($T_{rev}/2$), respectively. These revival times are characteristics of the molecular system itself, so we used them to calibrate the measured time delays in the experiment, as is already done in Fig. 2(b). From the fitting curve, the full revival signal around T_{rev} shows a minimum (the anti-alignment peak) at $T_{rev}^{\min} = 8.181$ ps and a maximum (the maximal alignment peak) at $T_{rev}^{max} = 8.336$ ps. As an inverse signal of the full revival, the half revival around $T_{rev}/2$ shows a maximum (the maximal alignment) at $T_{rev/2}^{max} = 3.991$ ps and a minimum (the anti-alignment peak) at $T_{rev/2}^{\min} = 4.145$ ps.

After obtaining experimental alignment signatures, we can infer the aligning pump intensity and initial rotational temperature before excitation from the occurrence times for the local alignment and anti-alignment peaks. When the time interval between the local maxima and local minima peaks increases, we expect the energies of the excited states be lower [44]. On the other hand, the final population depends on the aligning intensity. It also depends on the initial distribution of the rotational states, so the width of the revival and the time interval between its extrema is affected by the initial temperature [44].

The white light generation is mainly due to two effects: self-focusing and self-phase modulation [39], since they lead to spectral broadening due to dependence of the refractive index of the medium on the intensity of the propagating laser field. Thus, both these effects depend on the induced nonlinear refractive index n_2. If the signal of the white light is $S(n_2)$, then the molecular alignment introduces a variation of the nonlinear refractive index Δn, resulting in the variation of the white light signal $S(n_2 + \Delta n) - S(n_2) \approx (\partial S/\partial n_2)\Delta n$, which should be a good approximation, since the induced variation of the refractive index is quite small (on the order of 10^{-5}, see the scale factor in Fig. 2(a)). Thus, the observed variations of the measured white light that depend on the pump-probe delay are proportional to the variation of the refractive index induced by the alignment.

To extract the values of I and T from the measurements, we calculated the temporal evolution of the refractive index change Δn as a function of the aligning pump intensity and the initial rotational temperature according to Eqs. (2), (4). In Fig. 3(a) and 3(b), we plotted the occurrence times of the local alignment ($T_{rev/2}^{max}$) and anti-alignment ($T_{rev/2}^{\min}$) around $T_{rev/2} = 4.1ps$ as a function of the aligning intensity and initial rotational temperature. As these parameters increase, the occurrence time $T_{rev/2}^{max}$ is delayed, as seen in Fig. 3(a). On the other hand, $T_{rev/2}^{\min}$ shows an inverse dependence, since it reduces, as the aligning intensity and the rotational temperature increase (Fig. 3(b)). Also, the width of the revival is becoming smaller, when the aligning intensity and the rotational temperature increase. All the combinations of the pump intensities and rotational temperatures from the colormap of Fig. 3(a) that lead to the experimentally determined value of $T_{rev/2}^{max} = 3.991$ ps correspond to a contour line of a certain color, which is illustrated as the black dashed line in Fig. 3(a) and as the red solid line in Fig. 3(c). We have also chosen all the combinations of the aligning intensities and rotational temperatures from the colormap in Fig. 3(b) for the experimental value $T_{rev/2}^{min} = 4.145$ ps. The corresponding contour line is shown as the black dashed line in Fig. 3(b) and as the blue solid line in Fig. 3(c). From the resulting intersection of the lines in Fig. 3(c) the values of the aligning intensity and the initial rotational temperature are determined to be $I = 3.48 \times 10^{13}$ W/cm^2 and $T = 292.5$ K.

In Fig. 4(a) and 4(b), similarly, we plotted the occurrence times of the local alignment (T_{rev}^{max}) and local anti-alignment ($T_{rev}^{\min}$) extrema around $T_{rev} = 8.3$ ps as a function of the pump intensity and rotational temperature. The plot of Fig. 4(a) shows that when the aligning intensity and the initial rotational temperature increase, T_{rev}^{max} increases too. The plot for $T_{rev}^{\min}$ Fig. 4(b) shows the opposite dependence, namely, $T_{rev}^{\min}$ is decreasing with the increasing pump intensity and the rotational temperature. Note, that the results for the full revival T_{rev} exhibit a reversed behavior, compared to the half revival $T_{rev/2}$. From the colormaps of Fig. 4(a,b) we again select all the combinations of the pump intensities and rotational temperatures that lead to experimentally determines values $T_{rev}^{min} = 8.181$ ps and $T_{rev}^{max} = 8.336$ ps. These combinations are shown as dashed lines in Fig. 4(a,b) and lie on the blue (for $T_{rev}^{\min}$) and red (for T_{rev}^{max}) solid lines in Fig. 4(c). The resulting intersection gives the values for the pump intensity and rotational temperature, $I = 3.33 \times 10^{13}$ W/cm^2 and $T = 293.9$ K, respectively.

The main contribution to the uncertainty in the determination of temperature and intensity comes from the experimental error in the determination of temporal shifts of the respective minima and maxima relative to $T_{rev/2}$ and T_{rev} in the alignment signature. These positions can be determined with an uncertainty of ~3fs. To estimate the possible errors in obtained values of T and I, we can write $\Delta T = (\partial T/\partial t)\Delta t$ and $\Delta I = (\partial I/\partial t)\Delta t$. The values of the derivatives can be determined from calculations of Figs. 3, 4. We note that Figs. 3(a) and 4(a) give smaller errors in the determination of the intensity, while Figs. 3(b) and 4(b) give smaller uncertainty for temperature. The values of T and I obtained from half revival and full revival are close. Consequently, the values with uncertainties can be presented as $T = (293 \pm 20)$ K and $I = (3.4 \pm 0.8) \times 10^{13}$ W/cm^2. The value for the intensity that we calculated from the measured average power of the laser beam of 0.30 W is $I = 2.23 \times 10^{13}$ W/cm^2 and somewhat lower than the average value obtained from the alignment with the described procedure.

3. Conclusion

We performed in-situ measurement of aligning intensity and rotational temperature in the field-free molecular alignment of femtosecond laser pulses via white light generation in N_2 molecules. We derived the aligning intensity and initial rotational temperature using the occurrence times of the local alignment and anti-alignment extrema around the half and full revivals in the signals

obtained via white-light generation. The results proved that the intensity and initial rotational temperature is able to be obtained simultaneously by any two local alignment extrema showing contrary dependences on the aligning intensity and initial rotational temperature. This can be readily applied to other linear molecules to determine aligning intensity and initial rotational temperature with the field-free molecular alignment process.

Declaration of Competing Interest

The authors declare that they have no known competing financial interests or personal relationships that could have appeared to influence the work reported in this paper.

Acknowledgments

This work was supported by the Robert A. Welch Foundation Grant No. A1546 and the Scientific and Technological Research Council of Turkey (TÜBİTAK), Project No: 120F002.

References

[1] J. Küpper, S. Stern, L. Holmegaard, F. Filsinger, A. Rouzée, A. Rudenko, P. Johnsson, A.V. Martin, M. Adolph, A. Aquila, S. Bajt, A. Barty, C. Bostedt, J. Bozek, C. Caleman, R. Coffee, N. Coppola, T. Delmas, S. Epp, B. Erk, L. Foucar, T. Gorkhover, L. Gumprecht, A. Hartmann, R. Hartmann, G. Hauser, P. Holl, A. Hömke, N. Kimmel, F. Krasniqi, K.-U. Kühnel, J. Maurer, M. Messerschmidt, R. Moshammer, C. Reich, B. Rudek, R. Santra, I. Schlichting, C. Schmidt, S. Schorb, J. Schulz, H. Soltau, J.C.H. Spence, D. Starodub, L. Strüder, J. Thøgersen, M.J.J. Vrakking, G. Weidenspointner, T.A. White, C. Wunderer, G. Meijer, J. Ullrich, H. Stapelfeldt, D. Rolles, H.N. Chapman, X-ray diffraction from isolated and strongly aligned gas-phase molecules with a free-electron laser, Phys. Rev. Lett. 112 (2014), 083002.
[2] C.J. Hensley, J. Yang, M. Centurion, Imaging of isolated molecules with ultrafast electron pulses, Phys. Rev. Lett. 109 (2012), 133202.
[3] J. Itatani, J. Levesque, D. Zeidler, H. Niikura, H. Pépin, J.C. Kieffer, P.B. Corkum, D.M. Villeneuve, Tomographic imaging of molecular orbitals, Nature 432 (2004) 867–871.
[4] J. Yao, G. Li, X. Jia, X. Hao, B. Zeng, C. Jing, W. Chu, J. Ni, H. Zhang, H. Xie, C. Zhang, Z. Zhao, J. Chen, X. Liu, Y. Cheng, Z. Xu, Alignment-dependent fluorescence emission induced by tunnel ionization of carbon dioxide from lower-lying orbitals, Phys. Rev. Lett. 111 (2013), 133001.
[5] H. Xie, G. Li, J. Yao, W. Chu, Z. Chen, Y. Cheng, Intensity-independent molecular rotational decoherence lifetimes measured with mean wavelength shifts of femtosecond pulses, Chin. Opt. Lett. 16 (2018), 120201.
[6] Z. Liu, J. Yao, J. Chen, B. Xu, W. Chu, Y. Cheng, Near-resonant raman amplification in the rotational quantum wave packets of nitrogen molecular ions generated by strong field ionization, Phys. Rev. Lett. 120 (2018), 083205.
[7] H. Stapelfeldt, T. Seideman, Colloquium: aligning molecules with strong laser pulses, Rev. Mod. Phys. 75 (2003) 543–557.
[8] T. Seideman, E. Hamilton, Nonadiabatic alignment by intense pulses. concepts, theory, and directions, in: P.R. Berman, C.C. Lin (Eds.), Advances In Atomic, Molecular, and Optical Physics, Academic Press, 2005, pp. 289–329.
[9] C. Vozzi, F. Calegari, E. Benedetti, J.P. Caumes, G. Sansone, S. Stagira, M. Nisoli, R. Torres, E. Heesel, N. Kajumba, J.P. Marangos, C. Altucci, R. Velotta, Controlling two-center interference in molecular high harmonic generation, Phys. Rev. Lett. 95 (2005), 153902.
[10] M. Meckel, D. Comtois, D. Zeidler, A. Staudte, D. Pavičić, H.C. Bandulet, H. Pépin, J.C. Kieffer, R. Dörner, D.M. Villeneuve, P.B. Corkum, Laser-induced electron tunneling and diffraction, Science 320 (2008) 1478–1482.
[11] C. Vozzi, M. Negro, F. Calegari, G. Sansone, M. Nisoli, S. De Silvestri, S. Stagira, Generalized molecular orbital tomography, Nat. Phys. 7 (2011) 822–826.
[12] C. Zhai, X. Zhang, X. Zhu, L. He, Y. Zhang, B. Wang, Q. Zhang, P. Lan, P. Lu, Single-shot molecular orbital tomography with orthogonal two-color fields, Opt. Express 26 (2018) 2775–2784.
[13] C.Z. Bisgaard, O.J. Clarkin, G. Wu, A.M.D. Lee, O. Geßner, C.C. Hayden, A. Stolow, Time-resolved molecular frame dynamics of fixed-in-space CS2 molecules, Science 323 (2009) 1464–1468.
[14] L. Holmegaard, J.L. Hansen, L. Kalhoj, S. Louise Kragh, H. Stapelfeldt, F. Filsinger, J. Kupper, G. Meijer, D. Dimitrovski, M. Abu-samha, C.P.J. Martiny, L. Bojer Madsen, Photoelectron angular distributions from strong-field ionization of oriented molecules, Nat. Phys. 6 (2010) 428–432.
[15] J.L. Hansen, H. Stapelfeldt, D. Dimitrovski, M. Abu-samha, C.P.J. Martiny, L.B. Madsen, Time-resolved photoelectron angular distributions from strong-field ionization of rotating naphthalene molecules, Phys. Rev. Lett. 106 (2011), 073001.
[16] E. Gershnabel, I.S. Averbukh, Deflection of field-free aligned molecules, Phys. Rev. Lett. 104 (2010), 153001.
[17] S. Henrik, Laser aligned molecules: applications in physics and chemistry, Phys. Scr. 2004 (2004) 132.
[18] S. Fleischer, I.S. Averbukh, Y. Prior, Isotope-selective laser molecular alignment, Phys. Rev. A 74 (2006), 041403.
[19] R.J. Gordon, L. Zhu, W.A. Schroeder, T. Seideman, Nanolithography using molecular optics, J. Appl. Phys. 94 (2003) 669–676.
[20] R.A. Bartels, T.C. Weinacht, N. Wagner, M. Baertschy, C.H. Greene, M.M. Murnane, H.C. Kapteyn, Phase modulation of ultrashort light pulses using molecular rotational wave packets, Phys. Rev. Lett. 88 (2002), 013903.
[21] J. Wu, H. Cai, H. Zeng, A. Couairon, Femtosecond filamentation and pulse compression in the wake of molecular alignment, Opt. Lett. 33 (2008) 2593–2595.
[22] K.F. Lee, D.M. Villeneuve, P.B. Corkum, E.A. Shapiro, Phase control of rotational wave packets and quantum information, Phys. Rev. Lett. 93 (2004), 233601.
[23] P.M. Kraus, B. Mignolet, D. Baykusheva, A. Rupenyan, L. Horný, E.F. Penka, G. Grassi, O.I. Tolstikhin, J. Schneider, F. Jensen, L.B. Madsen, A.D. Bandrauk, F. Remacle, H.J. Wörner, Measurement and laser control of attosecond charge migration in ionized iodoacetylene, Science 350 (2015) 790–795.
[24] N. Hay, R. Velotta, M. Lein, R. de Nalda, E. Heesel, M. Castillejo, J.P. Marangos, High-order harmonic generation in laser-aligned molecules, Phys. Rev. A 65 (2002), 053805.
[25] J. Itatani, D. Zeidler, J. Levesque, M. Spanner, D.M. Villeneuve, P.B. Corkum, Controlling high harmonic generation with molecular wave packets, Phys. Rev. Lett. 94 (2005), 123902.
[26] S. Ramakrishna, T. Seideman, Information content of high harmonics generated from aligned molecules, Phys. Rev. Lett. 99 (2007), 113901.
[27] B. Wang, L. He, Y. He, Y. Zhang, R. Shao, P. Lan, P. Lu, All-optical measurement of high-order fractional molecular echoes by high-order harmonic generation, Opt. Express 27 (2019) 30172–30181.
[28] Y. He, L. He, P. Lan, B. Wang, L. Li, X. Zhu, W. Cao, P. Lu, Direct imaging of molecular rotation with high-order-harmonic generation, Phys. Rev. A 99 (2019), 053419.
[29] S.M. Purcell, P.F. Barker, Tailoring the optical dipole force for molecules by field-induced alignment, Phys. Rev. Lett. 103 (2009), 153001.
[30] S.M. Purcell, P.F. Barker, Controlling the optical dipole force for molecules with field-induced alignment, Phys. Rev. A 82 (2010), 033433.
[31] X.N. Sun, B.G. Jin, L.Y. Kim, B.J. Kim, B.S. Zhao, Strong optical dipole force exerted on molecules having low rotational temperature, ChemPhysChem 17 (2016) 3701–3708.
[32] F. Calegari, C. Vozzi, S. Gasilov, E. Benedetti, G. Sansone, M. Nisoli, S. De Silvestri, S. Stagira, Rotational Raman effects in the wake of optical filamentation, Phys. Rev. Lett. 100 (2008), 123006.

[33] J. Wu, H. Cai, Y. Peng, Y. Tong, A. Couairon, H. Zeng, Control of femtosecond filamentation by field-free revivals of molecular alignment, Laser Phys. 19 (2009) 1759–1768.
[34] H. Cai, J. Wu, Y. Peng, H. Zeng, Comparison study of supercontinuum generation by molecular alignment of N_2 and O_2, Opt. Express 17 (2009) 5822–5828.
[35] F. Calegari, C. Vozzi, S. Stagira, Optical propagation in molecular gases undergoing filamentation-assisted field-free alignment, Phys. Rev. A 79 (2009), 023827.
[36] Y. Wang, X. Dai, J. Wu, L. e Ding, H. Zeng, Spectral modulation of ultraviolet femtosecond laser pulse by molecular alignment of CO_2, O_2, and N_2, Appl. Phys. Lett. 96 (2010), 031105.
[37] S. Varma, Y.H. Chen, J.P. Palastro, A.B. Fallahkair, E.W. Rosenthal, T. Antonsen, H.M. Milchberg, Molecular quantum wake-induced pulse shaping and extension of femtosecond air filaments, Phys. Rev. A 86 (2012), 023850.
[38] J. Kasparian, M. Rodriguez, G. Méjean, J. Yu, E. Salmon, H. Wille, R. Bourayou, S. Frey, Y.B. Andre, A. Mysyrowicz, R. Sauerbrey, J.P. Wolf, L. Wöste, White-light filaments for atmospheric analysis, Science 301 (2003) 61–64.
[39] V.P. Kandidov, O.G. Kosareva, I.S. Golubtsov, W. Liu, A. Becker, N. Akozbek, C.M. Bowden, S.L. Chin, Self-transformation of a powerful femtosecond laser pulse into a white-light laser pulse in bulk optical media (or supercontinuum generation), Appl. Phys. B 77 (2003) 149–165.
[40] S.L. Chin, S.A. Hosseini, W. Liu, Q. Luo, F. Théberge, N. Aközbek, A. Becker, V.P. Kandidov, O.G. Kosareva, H. Schroeder, The propagation of powerful femtosecond laser pulses in opticalmedia: physics, applications, and new challenges, Can. J. Phys. 83 (2005) 863–905.
[41] A. Couairon, A. Mysyrowicz, Femtosecond filamentation in transparent media, Phys. Rep. 441 (2007) 47–189.
[42] E. Péronne, M.D. Poulsen, H. Stapelfeldt, C.Z. Bisgaard, E. Hamilton, T. Seideman, Nonadiabatic laser-induced alignment of iodobenzene molecules, Phys. Rev. A 70 (2004), 063410.
[43] E. Péronne, M.D. Poulsen, C.Z. Bisgaard, H. Stapelfeldt, T. Seideman, Nonadiabatic alignment of asymmetric top molecules: field-free alignment of iodobenzene, Phys. Rev. Lett. 91 (2003), 043003.
[44] V. Loriot, P. Tzallas, E.P. Benis, E. Hertz, B. Lavorel, D. Charalambidis, O. Faucher, Laser-induced field-free alignment of the OCS molecule, J. Phys. B At. Mol. Opt. Phys. 40 (2007) 2503–2510.
[45] Y. He, L. He, P. Wang, B. Wang, S. Sun, R. Liu, B. Wang, P. Lan, P. Lu, Measuring the rotational temperature and pump intensity in molecular alignment experiments via high harmonic generation, Opt. Express 28 (2020) 21182–21191.
[46] N. Kaya, G. Kaya, M. Sayrac, Y. Boran, S. Anumula, J. Strohaber, A. Kolomenskii, H. Schuessler, Probing nonadiabatic molecular alignment by spectral modulation, Opt. Express 24 (2016) 2562–2576.
[47] X.M. Tong, Z.X. Zhao, C.D. Lin, Theory of molecular tunneling ionization, Phys. Rev. A 66 (2002), 033402.
[48] J. Ortigoso, M. Rodríguez, M. Gupta, B. Friedrich, Time evolution of pendular states created by the interaction of molecular polarizability with a pulsed nonresonant laser field, J. Chem. Phys. 110 (1999) 3870–3875.
[49] B. Friedrich, D. Herschbach, Alignment and trapping of molecules in intense laser fields, Phys. Rev. Lett. 74 (1995) 4623–4626.
[50] B. Friedrich, D. Herschbach, Enhanced orientation of polar molecules by combined electrostatic and nonresonant induced dipole forces, J. Chem. Phys. 111 (1999) 6157–6160.
[51] D.A. McQuarrie, J.D. Simon. Physical Chemistry: A Molecular Approach, University Science Books, 1997.